

# Dislocation as a bulk probe of higher-order topological insulators

Bitan Roy<sup>1,\*</sup> and Vladimir Juričić<sup>2,†</sup>

<sup>1</sup>*Department of Physics, Lehigh University, Bethlehem, Pennsylvania, 18015, USA*

<sup>2</sup>*Nordita, KTH Royal Institute of Technology and Stockholm University, Roslagstullsbacken 23, 10691 Stockholm, Sweden*

(Dated: December 19, 2021)

Topological materials occupy the central stage in the modern condensed matter physics because of their robust metallic edge or surface states protected by the topological invariant, characterizing the electronic band structure in the bulk. Higher order topological (HOT) states extend this usual bulk-boundary correspondence, so they host the modes localized at lower-dimensional boundaries, such as corners and hinges, which may hinder their experimental detection. Here, we theoretically demonstrate that dislocations, ubiquitous defects in crystalline materials, can probe higher-order topology, recently realized in various platforms, such as crystalline, phononic, photonic, topoelectric, and artificial lattice systems. As we show, HOT insulators respond to a dislocation defect through the protected finite-energy in-gap modes, localized at the defect core in the bulk of a second-order topological insulator. Our findings are consequential for the systematic probing of the extended bulk-boundary correspondence in a broad range of HOT crystals and metamaterials through the bulk topological lattice defects, controllable in state-of-the-art experiments.

The nontrivial topological invariant characterizing the bulk electronic band structure gives rise to the robust edge or surface modes, manifesting the hallmark feature of a topological material - the bulk-boundary correspondence [1, 2]. As such, these boundary modes have been so far almost exclusively used to experimentally detect nontrivial electronic topology, both in gapped [3–8] and gapless [9, 10] systems. Equally important, but much less explored, is direct probing of topological states in the bulk without invoking the boundary modes, through the response of topological lattice defects, such as dislocations [11–17]. Moreover, the topological modes bound to the defect core in the bulk of the system are more pristine and should be easier to detect as they avoid contamination by the interfaces. In fact, in the context of experimental probing of topology in the quantum materials this aspect has started to gain prominence recently [18, 19].

In  $D$ -dimensional  $n$ th order topological states [20–24], bulk probing of the electronic band topology should play a specially important role, because the extended bulk-boundary correspondence is realized through gapless modes on the lower,  $(D - n)$ -dimensional boundaries, characterized by codimension  $d_c = D - n$ , such as hinges ( $d_c = D - 1$ ) and corners ( $d_c = D$ ) [25–31]. These robust modes on lower-dimensional boundaries may be thought of as inherited from the parent, first-order topological state (with  $n = 1$ ) upon partially gapping out its edge or surface modes ( $d_c = 1$ ), which can, in turn, yield a hierarchical ladder of HOT states [32]. The gap is realized by a suitable domain wall mass which changes sign across corners or hinges, thus localizing topological modes at these lower-dimensional boundaries. The reduced dimensionality of the boundary may, however, hinder the experimental detection of the gapless modes, and therefore HOT states require other means to directly probe the bulk electronic topology.

As we show here, dislocations can serve as bulk probes

of HOT insulators through binding of the special topologically protected modes, see Figs. 1 and 2. To formulate the mechanism, we recall that a dislocation in a two-dimensional (2D) lattice can be created by removing a line ending at a lattice site, the dislocation center, and reconnecting the sites across the removed line so that the translational symmetry is restored away from the defect center, see Fig. 1(a). Therefore, any closed loop around the dislocation center features a missing translation by the Burgers vector  $\mathbf{b}$ , which topologically characterizes the defect. As such, a dislocation provides global frustration to the underlying crystalline order. In turn, this translates into a nontrivial effect on the electrons moving on the lattice. Namely, an electron with a momentum  $\mathbf{K}$  when encircling the dislocation picks up a phase equal to  $\exp[i\Phi_{\text{dis}}]$ , with  $\Phi_{\text{dis}} = \mathbf{K} \cdot \mathbf{b} \pmod{2\pi}$ . In particular, for topological states with the band inversion momentum at  $\mathbf{K}_{\text{inv}}$ , the hopping phase is  $\Phi_{\text{dis}} = \mathbf{K}_{\text{inv}} \cdot \mathbf{b} \pmod{2\pi}$  [11].

In a first-order 2D topological insulator, such as the quantum spin Hall insulator (QSHI) with band inversion at a non- $\Gamma$  point in the Brillouin zone (BZ), the defect effectively acts as an antiphase boundary ( $\Phi_{\text{dis}} = \pi$ ) for the gapless helical edge modes. Consequently, it yields a Kramers pair of zero-energy bound states [13]. In contrast, HOT states feature *gapped* edge states that stem from the mass domain wall in the bulk gapping out the edge states, and possibly obstructing the formation of the localized dislocation modes. However, the domain wall gaps out the surface only *partially* in turn producing the topological corner modes through the Jackiw-Rebbi mechanism [33]. Consequently, the dislocation modes, originating from the edge states across the antiphase boundary, still survive but are moved away from zero energy [Figs. 1(b),(c)]. Importantly, when the orientation of the Burgers vector ( $\mathbf{b}$ ) is parallel to the direction of the domain wall, the dislocation modes are pinned at zero energy [Fig. 1(d)]. Hierarchy of HOT states in

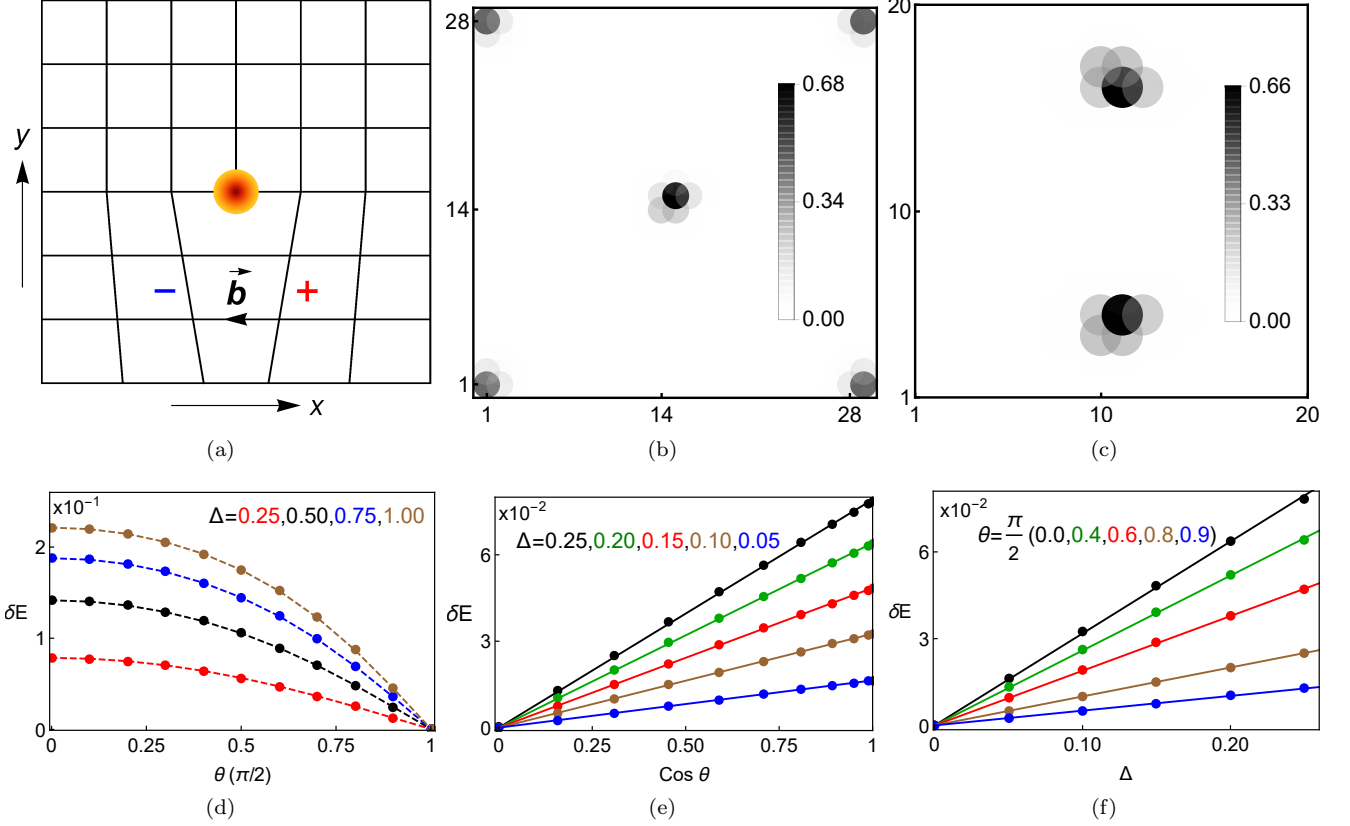


FIG. 1: Dislocation defect in a square lattice. (a) The defect is obtained through the Volterra cut-and-glue procedure by removing a line of atoms ending at the center of the lattice (orange) and reconnecting the edges denoted by + and -, right and left from the center, respectively. The corresponding Burgers vector is  $\mathbf{b} = -ae_x$ . (b) LDOS for the dislocation mode localized at the defect core together with the four corner modes in a second-order translationally-active HOT insulator with the band inversion at the  $M$  point of the BZ ( $t = t_0 = m = 1$  and  $\Delta = 0.25$ ). Here, we set  $\theta = 0$  in the model given by Eq. (1) so that the defect modes are at finite energies, while the four corner modes are at zero energy. (c) LDOS for the zero-energy dislocation modes in the periodic system with two dislocations for  $\theta = 0$ . (d) The scaling of the spectral gap ( $\delta E$ ) among four states localized at the core of the dislocation with  $\theta$  measuring the orientation of the four-fold symmetry breaking mass domain wall. Note that these modes become zero-energy states as  $\theta \rightarrow \pi/2$ , when the Burgers vector becomes parallel to one of the four-fold symmetry breaking axes. The various choices of the amplitude of the  $C_4$  symmetry breaking mass ( $\Delta$ ) are quoted in the figure (the rest of the parameters are unchanged). For small  $\Delta$ , the spectral gap ( $\delta E$ ) scales *linearly* with (e)  $\cos \theta$  and (f)  $\Delta$ .

this way directly translates into the spectral flow of the defect modes, detectable in the tunneling spectroscopy measurements, for instance. Finally, the same mechanism is analogously operative for three-dimensional (3D) HOT insulators as the dislocation line defects in their parent first-order states may feature gapless propagating modes.

To show the outlined general mechanism, we first analyze the minimal model describing a 2D second-order insulator, with the Hamiltonian  $H = \sum_{\mathbf{k}} \Psi_{\mathbf{k}}^\dagger \hat{h} \Psi_{\mathbf{k}}$ , where  $\hat{h} = \hat{h}_0 + \hat{h}_\Delta$ , and

$$\begin{aligned} \hat{h}_0 &= t [\sin(k_x a) \Gamma_1 + \sin(k_y a) \Gamma_2] \\ &+ \{m + t_0 [\cos(k_x a) + \cos(k_y a)]\} \Gamma_3, \\ \hat{h}_\Delta &= \Delta \{ \cos \theta [\cos(k_x a) - \cos(k_y a)] \} \\ &+ \sin \theta \sin(k_x a) \sin(k_y a) \} \Gamma_4. \end{aligned} \quad (1)$$

$$\text{Here, the spinor } \Psi_{\mathbf{k}} = (c_{A,\uparrow}^{\mathbf{k}}, c_{B,\uparrow}^{\mathbf{k}}, c_{A,\downarrow}^{\mathbf{k}}, c_{B,\downarrow}^{\mathbf{k}})^\top, \text{ with } c_{X,\sigma}^{\mathbf{k}} \text{ as the annihilation operator acting on the two sublattices } X = A, B, \text{ and spin projections } \sigma = \uparrow, \downarrow, \text{ while } \mathbf{k} \text{ is the momentum, and } a \text{ is the lattice spacing. The mutually anticommuting four-component } \Gamma \text{ matrices are } \Gamma_1 = \tau_1 \otimes \sigma_3, \Gamma_2 = \tau_2 \otimes \sigma_0, \Gamma_3 = \tau_3 \otimes \sigma_0, \Gamma_4 = \tau_1 \otimes \sigma_1, \text{ and } \Gamma_5 = \tau_1 \otimes \sigma_2, \text{ with } \boldsymbol{\tau} \text{ and } \boldsymbol{\sigma} \text{ Pauli matrices acting in the sublattice and the spin spaces, respectively.}$$

This model for the regime of parameters  $|m/t_0| \leq 2$  describes a first-order QSHI and a 2D HOT insulator (second-order) for  $\Delta = 0$  and finite  $\Delta$ , respectively. Furthermore, when  $0 \leq m/t_0 \leq 2$ , the model features the band inversion at the  $M = (\pi/a, \pi/a)$  point (the  $M$  phase), while for  $-2 \leq m/t_0 \leq 0$ , the band inversion

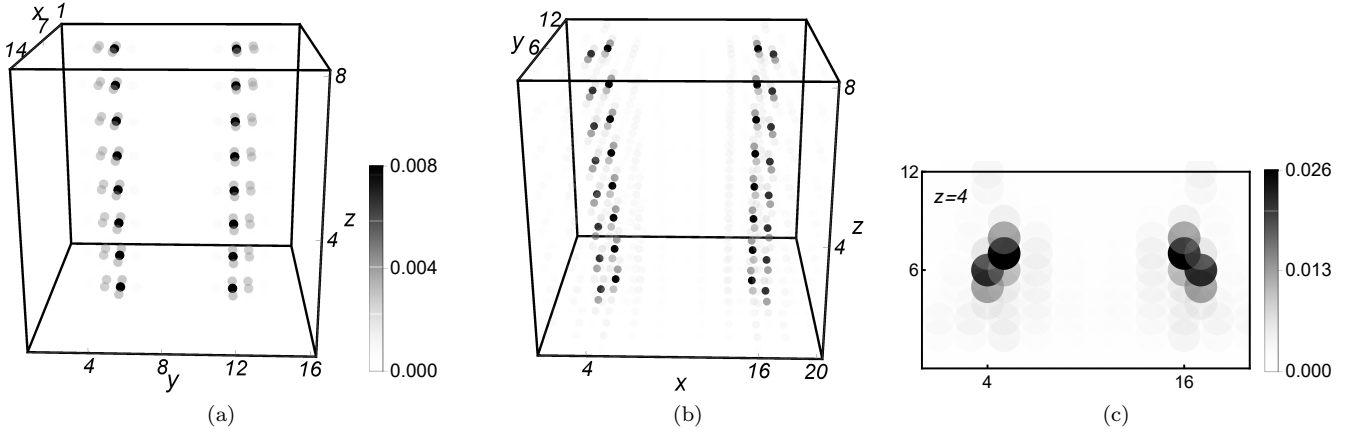


FIG. 2: Dislocation defect modes in a 3D HOT insulator on a cubic lattice. (a) LDoS for the closest to zero energy modes localized at an edge dislocation-antidislocation pair directed in the  $z$ -direction (hosting hinge modes in the open system) with the Burgers vectors  $\mathbf{b} = \pm \mathbf{e}_x$  in a second-order topological insulator with the band inversion at the  $R = (\pi/a, \pi/a, \pi/a)$  point of the BZ. (b) LDoS for the finite, but still closest to zero energy dislocation modes in the same HOT phase in the periodic system with a screw dislocation-antidislocation pair oriented in the  $z$ -direction, with  $\mathbf{b} = \pm a\mathbf{e}_z$ . (c) Corresponding LDoS at a particular  $z = 4$  plane explicitly showing that the localization of the modes to the defect core within a few lattice sites. Here, we set  $t = B = 1$ ,  $m = 10$ ,  $\Delta = 0.75$  in the model given by Eq. (5).

is at the  $\Gamma = (0, 0)$  point (the  $\Gamma$  phase) of the BZ. Notice that  $\{\hat{h}_0, \hat{h}_\Delta\} = 0$ , and therefore  $\hat{h}_\Delta$  acts as a mass term for the topological edge states of QSHI. This mass term changes sign under the  $C_4$  rotation and, as such, assumes the profile of a discrete symmetry breaking Wilson-Dirac mass, the exact form of which depends on the parameter  $\theta \in [0, \pi/2]$ . In particular, for  $\theta = \pi/2$  the domain wall lies along the diagonals  $k_y = \pm k_x$ , while for  $\theta = 0$  it is located along the principal axes,  $k_x = 0, k_y = 0$ .

We perform numerical analysis of the above model in the presence of a lattice dislocation defect with the Burgers vector  $\mathbf{b} = a\mathbf{e}_x$ , oriented in the lattice  $x$ -direction, see Fig. 1(a). We arrive at the same conclusions when the Burgers vector is  $\mathbf{b} = a\mathbf{e}_y$ . The tight-binding Hamiltonian given by Eq. (1) is implemented in the real space on a square lattice. We focus on the translationally-active HOT  $M$  phase in which the dislocation, as previously discussed, provides  $\pi$  phase factor upon encircling it. In an open system, the dislocation modes and the corner states coexist in the HOT  $M$  phase, explicitly showing that the defect can probe the extended bulk-boundary correspondence, see Fig. 1(b). Furthermore, we find that dislocations host the modes in a lattice without boundaries (periodic boundary conditions), further corroborating their role as a bulk probe of higher-order electronic topology, as displayed in Fig. 1(c). The hybridization effects in both cases can be neglected as the defect modes are localized within a few lattice sites around its center, which is much shorter than both the system size and the separation between the defects.

Most importantly, for any choice of the domain wall orientation ( $\theta$ ), we find that the defects feature mid-gap

bound states at *finite* energies, see Fig. 1(d). As the domain wall orientation approaches the direction of the Burgers vector, i.e.  $\theta \rightarrow \pi/2$ , the energy gap between the dislocation modes decreases. Eventually, when the directions of the domain wall and Burgers vector are parallel ( $\theta = \pi/2$ ), the energy splitting between the defect modes vanishes, and they become zero energy states. The scaling of the spectral gap ( $\delta E$ ) among the defect modes with the domain wall orientation ( $\theta$ ) for various choices of the Wilson-Dirac mass parameter  $\Delta$  is shown in Fig. 1(d). It can be clearly seen that the gap vanishes as  $\theta \rightarrow \pi/2$  for any value of  $\Delta$ .

We now provide an analytical argument for the above numerically observed dislocation modes in the HOT  $M$  phase. To this end, we take a dislocation with the Burgers vector  $\mathbf{b} = a\mathbf{e}_x$  and the Hamiltonian in Eq. (1) close to the bandgap closing at the  $M$  point. In the continuum limit, for  $\Delta = 0$  in the real space we then obtain

$$\hat{h}_M = it\Gamma_1\partial_x + it\Gamma_2\partial_y - \Gamma_3 \left[ \tilde{m} + \tilde{B}(\partial_x^2 + \partial_y^2) \right], \quad (2)$$

where in the  $M$  phase  $\tilde{m} = -(m - 2t_0) > 0$ ,  $\tilde{B} = t_0/2 > 0$ , and we conveniently set  $a = 1$ .

A dislocation is created by removing a line of sites ending at  $\mathbf{r}_{\text{dis}} = (0, 0)$  (the center of the lattice). The two edges along the lines  $x_\pm = \pm a$  [Fig. 1(a)], before they are reconnected, feature topological gapless edge states, resulting from the corresponding zero modes of the edge Hamiltonian  $H_{\text{edge}} = [it\Gamma_1\partial_x - (\tilde{m} + \tilde{B}\partial_x^2)\Gamma_3] \otimes \mu_3$ , where the Pauli matrices  $\mu$  act in the space of the two edges. The reconnection of the edges is modeled by a hopping Hamiltonian between them in the form  $H_D = t \text{sgn}(x)\Gamma_1 \otimes \mu_1$ , where  $\text{sgn}(x)$  is the sign func-

tion. This term takes into account that the (low-energy) electrons acquire a nontrivial  $\pi$  phase around the dislocation defect and it preserves the form of the hopping in the sublattice and spin space in the direction of the Burgers vector. We then find that the Hamiltonian  $H_{\text{edge}} + H_{\text{D}}$  features a pair of the zero energy dislocation modes given by

$$\Psi_0^{(1,2)}(x) = \mathcal{C}\chi_{\text{sgn}(x)}^{(1,2)} \otimes \varphi_{\pm 1} \left( e^{-\lambda_1|x|} - e^{-\lambda_2|x|} \right). \quad (3)$$

Here, the spinors are the eigenstates with eigenvalues  $\sigma, \rho = \pm 1$  of the operators  $i\Gamma_1\Gamma_3$  and  $\mu_2$ , respectively, since both of them *anticommute* with  $H_{\text{edge}} + H_{\text{D}}$ ,

$$i\Gamma_1\Gamma_3\chi_{\sigma}^{(1,2)} = \sigma\chi_{\sigma}^{(1,2)}, \quad \mu_2\varphi_{\rho} = \rho\varphi_{\rho}, \quad (4)$$

and  $\lambda_{1,2} = [t \pm \sqrt{t^2 - 4\tilde{B}(M + \tilde{m})}]/(2\tilde{B})$ . We take  $t^2 > 4\tilde{B}(M + \tilde{m})$  close to the phase boundary between the  $M$  phase and trivial insulator, and the continuity of the wavefunction requires  $\Psi_0^{(1,2)}(x \rightarrow 0) = 0$  [see Supplementary Materials (SM) for details]. The solution in Eq. (4) is determined up to a localized function  $f(y)$  that fixes (regularization-dependent) form of the zero modes around the center of the dislocation. The latter detail is, however, irrelevant for the remainder of the analysis.

We now introduce the HOT mass term  $\hat{h}_{\Delta}$  [see Eq. (1)]. This term reduces in the subspace of the dislocation zero modes since  $[\Gamma_4, i\Gamma_1\Gamma_3] = 0$  and therefore *symmetrically* splits them about the zero energy. Furthermore, since the band inversion is at the  $M$  point and the Burgers vector is oriented in the  $x$ -direction, for the low-energy modes the components of the momentum are  $k_x = \pi/a + q_x$ ,  $k_y = \pi/a$ , with  $q_x = -i\partial_x$  due to the broken translational symmetry in the  $x$ -direction because of the defect. The energy splitting is then given by  $\delta E = 2\Delta \cos \theta \tilde{E}$ , where  $\tilde{E} \sim |\int dx (\Psi^{(1,2)})^{\dagger} \partial_x^2 \Psi^{(1,2)}|$ . Therefore, this argument captures the existence of the midgap dislocation modes in the  $M$  phase. In particular, the form of the energy gap we found yields the dislocation modes precisely at zero energy when the Burgers vector is parallel with the direction of the mass domain wall, corresponding to  $\theta = \pi/2$ , as shown in Fig. 1(d). Furthermore, for small  $\Delta$  the energy gap  $\delta E$  scales linearly with  $\cos \theta$  [see Fig. 1(e)] and  $\Delta$  [see Fig. 1(f)]. Finally, according to this argument, a dislocation does not feature any bound states neither in the  $\Gamma$  phase, nor in the trivial phase. In the former case, the phase factor across the edges is trivial, the reconnection Hamiltonian is thus  $H_{\text{D}} = t\Gamma_1 \otimes \mu_1$ , and they are just gapped out. By contrast, in the latter case no topological edge states even exist.

The above arguments can be straightforwardly extended to 3D HOT insulators, in particular when dislocation line defects are directed parallel to the hinges hosting propagating 1D gapless modes. As a result, such an *edge* dislocation with the Burgers vector parallel to the mass domain wall direction yields *gapless*, while its *screw*

counterpart always hosts *gapped* helical modes. To this end, notice that a 3D edge dislocation can be obtained from its 2D analogue by translating it along an out-of-plane lattice vector representing the dislocation direction in three dimensions. Therefore, an edge dislocation in a 3D second-order topological insulator should in general feature *gapped* helical modes localized in its core, which, however, become *gapless* for the Burgers vector oriented parallel to the mass domain wall direction (hosting hinge modes in the open system), analogously to the 2D case. A screw dislocation, being a true 3D defect, in a translationally-active HOT insulator acts as an antiphase domain wall when  $\mathbf{K}_{\text{inv}} \cdot \mathbf{b} = \pi \pmod{2\pi}$  between otherwise gapped surface states of the parent first-order topological insulator. As such, it can give rise to localized bound states at a finite energy (as shown in the SM), analogous to an edge dislocation in 2D HOT insulator, which in turn yield gapped one-dimensional modes due to translational symmetry along the defect line.

We now confirm this scenario in numerical simulations of a 3D second-order topological insulator described by the tight-binding Hamiltonian on the cubic lattice with the form analogous to Eq. (1), but with

$$\begin{aligned} h_0 &= t [\sin(k_x a)\Gamma_1 + \sin(k_y a)\Gamma_2 + \sin(k_z a)\Gamma_3] \\ &\quad + \{m - 2B [3 - \cos(k_x a) - \cos(k_y a) - \cos(k_z a)]\} \Gamma_4, \\ \hat{h}_{\Delta} &= \Delta \{ \cos \theta [\cos(k_x a) - \cos(k_y a)] \\ &\quad + \sin \theta \sin(k_x a) \sin(k_y a) \} \Gamma_5. \end{aligned} \quad (5)$$

For our numerical analysis, we consider the  $R$ -phase with the band inversion at the  $R = (\pi/a, \pi/a, \pi/a)$  point in the BZ, realized for the values of the parameters  $8 < m < 12$ ,  $t = 1$  and  $B = 1$ . An edge dislocation-antidislocation pair extending in the  $z$ -direction (hinge mode direction in an open system) with Burgers vectors  $\mathbf{b} = \pm a\mathbf{e}_x$ , in a second-order topological insulator in the  $R$ -phase with periodic boundary conditions (PBC) indeed yields finite energy states when  $\theta \neq \pi/2$ , as shown in Fig. 2(a). In the thermodynamic limit and for  $\theta = \pi/2$  these modes become gapless (same as in 2D), as explicitly shown in the SM. In the same topological phase, for a screw dislocation-antidislocation pair with  $\mathbf{b} = \pm a\mathbf{e}_z$ , we always obtain *gapped* dislocation modes (with PBC) close to zero energy, as displayed in Fig. 2(b). These modes are localized within a few lattice sites at the defect core, as can be seen from the LDoS in a plane perpendicular to the dislocation direction in Fig. 2(c).

Our findings are experimentally consequential for probing HOT insulators, apart from the crystalline systems, also in metamaterials. The paradigmatic model of the 2D second-order HOT insulator, the Benalcazar-Bernevig-Hughes (BBH) model [20], equivalent to the minimal lattice model in Eq. (1) [34], has been realized in the lattice of microwave resonators [27]. A dislocation defect in this setup should be created by a local hopping modification through  $\pi$  phase factors across a line of

missing sites ending at the dislocation center, analogously to the case of a weak (translationally-active) first-order topological insulator [35], and a disclination [36]. In the BBH photonic lattice, where the sign of the hopping also can be locally manipulated [37], it should be therefore possible to introduce the dislocation defects and observe the defect modes, as in a first-order 2D topological photonic crystals [38, 39], and for a disclination defect [40]. Finally, the artificial lattices can host HOT phases, as recently shown for Kagome lattice [31]. Since both the amplitude and signs of the hoppings can be controlled there, we expect that dislocation defects can also be engineered, and therefore our theoretical predictions can be directly tested in these platforms.

In 3D, elemental Bi exhibits mixed electronic topology manifesting through coexisting gapless hinge and Dirac surface modes [19, 25, 41]. Our results imply that an edge dislocation line along the (111) hinge direction with a Burgers vector oriented in one of the hexagonal bisectrix directions (see, Fig. 1c in Ref. [25]) should feature a gapless pair of propagating modes. Similarly, for recently proposed HOT insulator in  $Zr(TiH_2)_2$ , with band-inversion away from the  $\Gamma$  point and the gapless modes along all the edges in the cubic geometry [42], we predict gapless (gapped) modes in the core of an edge (a screw) dislocation defect with the Burgers vector along a principal crystal axis. Finally, the candidate HOT insulators  $Bi_4X_4$ , with  $X=Br,I$ , [42–45] feature band inversion at  $R$  and  $M = (\pi/a, \pi/a, 0)$  points in the BZ. Therefore the edge and screw dislocations in these compounds should host gapped and gapless propagating modes, depending on the precise orientation of the defect and the Burgers vector, following the above general rule.

In summary, we show that dislocation defects can be instrumental in probing the bulk topology of second-order topological insulators in both two and three dimensions. Similar conclusions should also hold for HOT semimetals [32, 46] and superconductors.

*Acknowledgment.* B.R. was supported by the Startup Grant from Lehigh University. V. J. acknowledges the support from the Swedish Research Council (VR 2019-04735).

- [6] D. Hsieh, *et. al.* *Science* **323**, 919 (2009).
- [7] Y. L. Chen, *et. al.* *Science* **325**, 178 (2009).
- [8] P. Dziawa, *et. al.* *Nat. Mater.* **11**, 1023 (2012).
- [9] S.-Y. Xu, *et. al.* *Science* **349**, 613 (2015).
- [10] B. Q. Lv, *et. al.* *Phys. Rev. X* **5**, 031013 (2015).
- [11] Y. Ran, Y. Zhang, and A. Vishwanath, *Nat. Phys.* **5**, 298 (2009).
- [12] J. C. Y. Teo and C. L. Kane, *Phys. Rev. B* **82**, 115120 (2010).
- [13] V. Jurićić, A. Mesaros, R.-J. Slager, and J. Zaanen, *Phys. Rev. Lett.* **108**, 106403 (2012).
- [14] D. Asahi and N. Nagaosa *Phys. Rev. B* **86**, 100504(R) (2012).
- [15] T. L. Hughes, H. Yao, and X.-L. Qi, *Phys. Rev. B* **90**, 235123 (2014).
- [16] R.-J. Slager, A. Mesaros, V. Jurićić, and J. Zaanen, *Phys. Rev. B* **90**, 241403(R) (2014).
- [17] Y. You, G. Y. Cho, and T. L. Hughes, *Phys. Rev. B* **94**, 085102 (2016).
- [18] H. Hamasaki, Y. Tokumoto, and K. Edagawa, *Appl. Phys. Lett.* **110**, 092105 (2017).
- [19] A. K. Nayak, *et. al.* *Sci. Adv.* **5**, eaax6996 (2019).
- [20] W. A. Benalcazar, B. A. Bernevig, and T. L. Hughes, *Science* **357**, 61 (2017).
- [21] W. A. Benalcazar, B. A. Bernevig, and T. L. Hughes, *Phys. Rev. B* **96**, 245115 (2017).
- [22] Z. Song, Z. Fang, and C. Fang, *Phys. Rev. Lett.* **119**, 246402 (2017).
- [23] J. Langbehn, Y. Peng, L. Trifunovic, F. von Oppen, and P. W. Brouwer, *Phys. Rev. Lett.* **119**, 246401 (2017).
- [24] F. Schindler, *et. al.* *Sci. Adv.* **4**, eaat0346 (2018).
- [25] F. Schindler, *et. al.* *Nat. Phys.* **14**, 918 (2018).
- [26] M. Serra-Garcia, *et. al.* *Nature* **555**, 342 (2018).
- [27] C. W. Peterson, W. A. Benalcazar, T. L. Hughes, and G. Bahl, *Nature* **555**, 346 (2018).
- [28] X. Ni, M. Weiner, A. B. Alu Khanikaev, *Nat. Mater.* **18**, 113 (2019).
- [29] X. Zhang, *et. al.* *Nat. Phys.* **15**, 582 (2019).
- [30] S. Imhof, *et. al.* *Nat. Phys.* **14**, 925 (2018).
- [31] S. N. Kempkes, *et. al.* *Nat. Mater.* **18**, 1292 (2019).
- [32] D. Călugăru, V. Jurićić, and B. Roy, *Phys. Rev. B* **99**, 041301(R) (2019).
- [33] R. Jackiw and C. Rebbi, *Phys. Rev. D* **13**, 3398 (1976).
- [34] B. Roy, *Phys. Rev. Research* **1**, 032048(R) (2019).
- [35] I. H. Grinberg, *et. al.* arXiv:1909.01431 (2019).
- [36] C. W. Peterson, *et. al.* arXiv:2004.11390 (2020).
- [37] S. Mittal, *et. al.* *Nat. Photonics* **13**, 692 (2019).
- [38] J. Noh, *et. al.* *Nat. Photonics* **12**, 408 (2018).
- [39] F. F. Li, *et. al.* *Nat. Comm.* **9**, 2462 (2018).
- [40] Y. Liu, *et. al.* arXiv:2003.08140 (2020).
- [41] C. H. Hsu, *et. al.* *PNAS* **119**, 13255 (2019).
- [42] T. Zhang, *et. al.* *Nature* **566**, 475 (2019).
- [43] M. G. Vergniory, *et. al.* *Nature* **566**, 480 (2019).
- [44] F. Tang, H. C. Po, A. Vishwanath and X. Wang, *Nature* **566**, 486 (2019).
- [45] C. Yoon, C. C. Liu, H. Min, and F. Zhang arXiv:2005.14710 (2020).
- [46] M. Lin and T. L. Hughes, *Phys. Rev. B* **98**, 241103(R) (2018).

\* Electronic address: bitan.roy@lehigh.edu

† Electronic address: vladimir.juricic@nordita.org

- [1] M. Z. Hasan and C. L. Kane, *Rev. Mod. Phys.* **82**, 3045 (2010).
- [2] X. L. Qi and S. C. Zhang, *Rev. Mod. Phys.* **83**, 1057 (2011).
- [3] M. König, *et. al.* *Science* **318**, 766 (2007).
- [4] D. Hsieh, *et. al.* *Nature* **452**, 970 (2008).
- [5] Y. Xia, *et al.* *Nat. Phys.* **5**, 398 (2009).